Supplemental Figure 1: Validation of first trimester TO and DO cultures

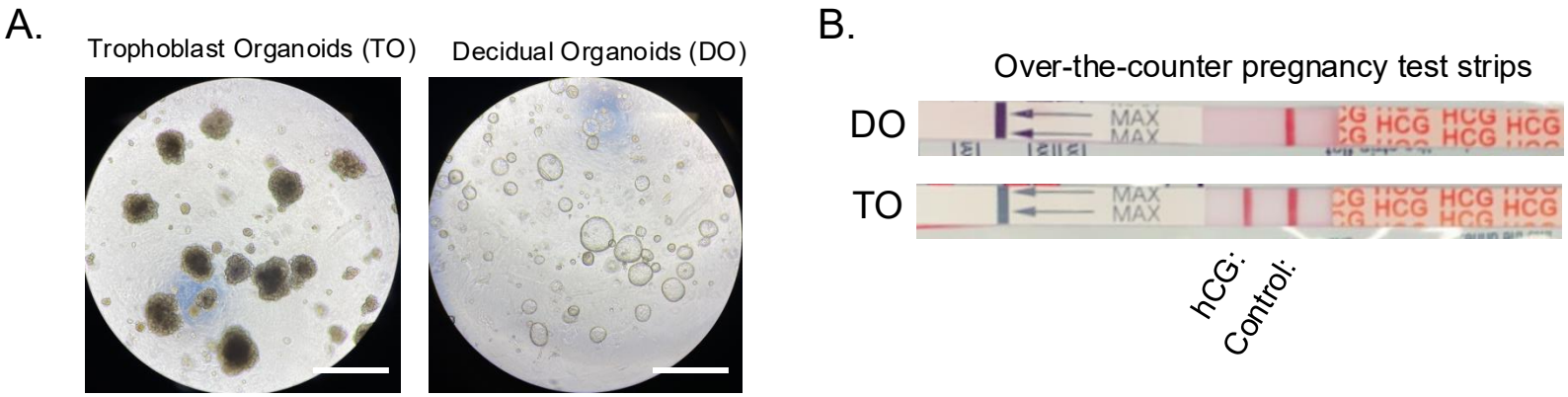

Supplemental Figure 1. Validation of first trimester TO and DO cultures

A. Representative brightfield images of TOs and DOs in culture. 5X magnification. Scale bar, 100μm.

B. Over the counter pregnancy test strips were used to detect secreted trophoblast-specific hormone hCG in TO- and DO-conditioned media.

Supplemental Figure 2: ZIKV infection of TO cultures

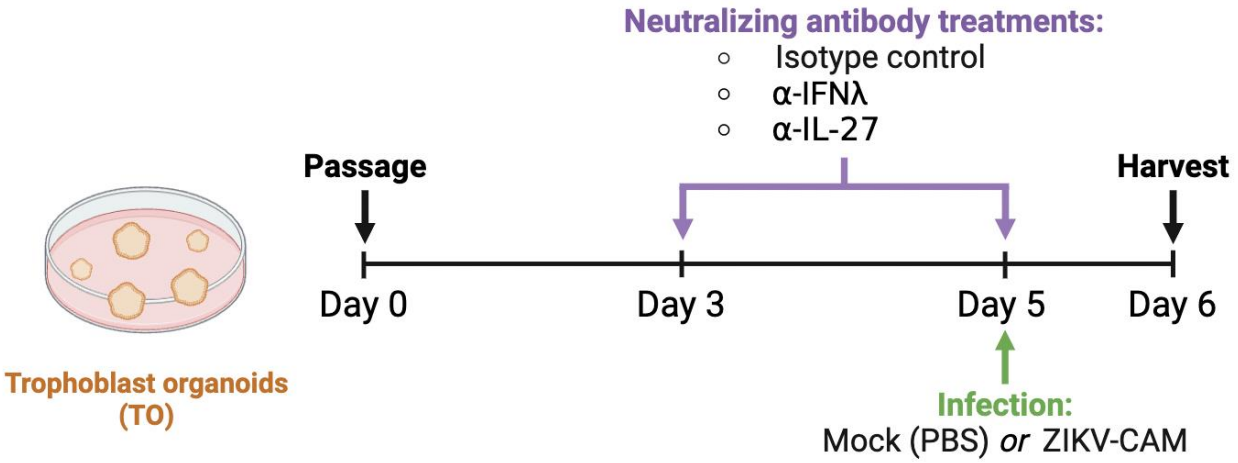

Supplemental Figure 2. ZIKV infection of TO cultures

A. Schematic of experimental design for TO infection with Cambodian ZIKV (ZIKV-CAMB) as quantified in **Figure 1E**. Graphics were created with Biorender.com.

Supplemental Figure 3. Bulk RNA-sequencing of TOs

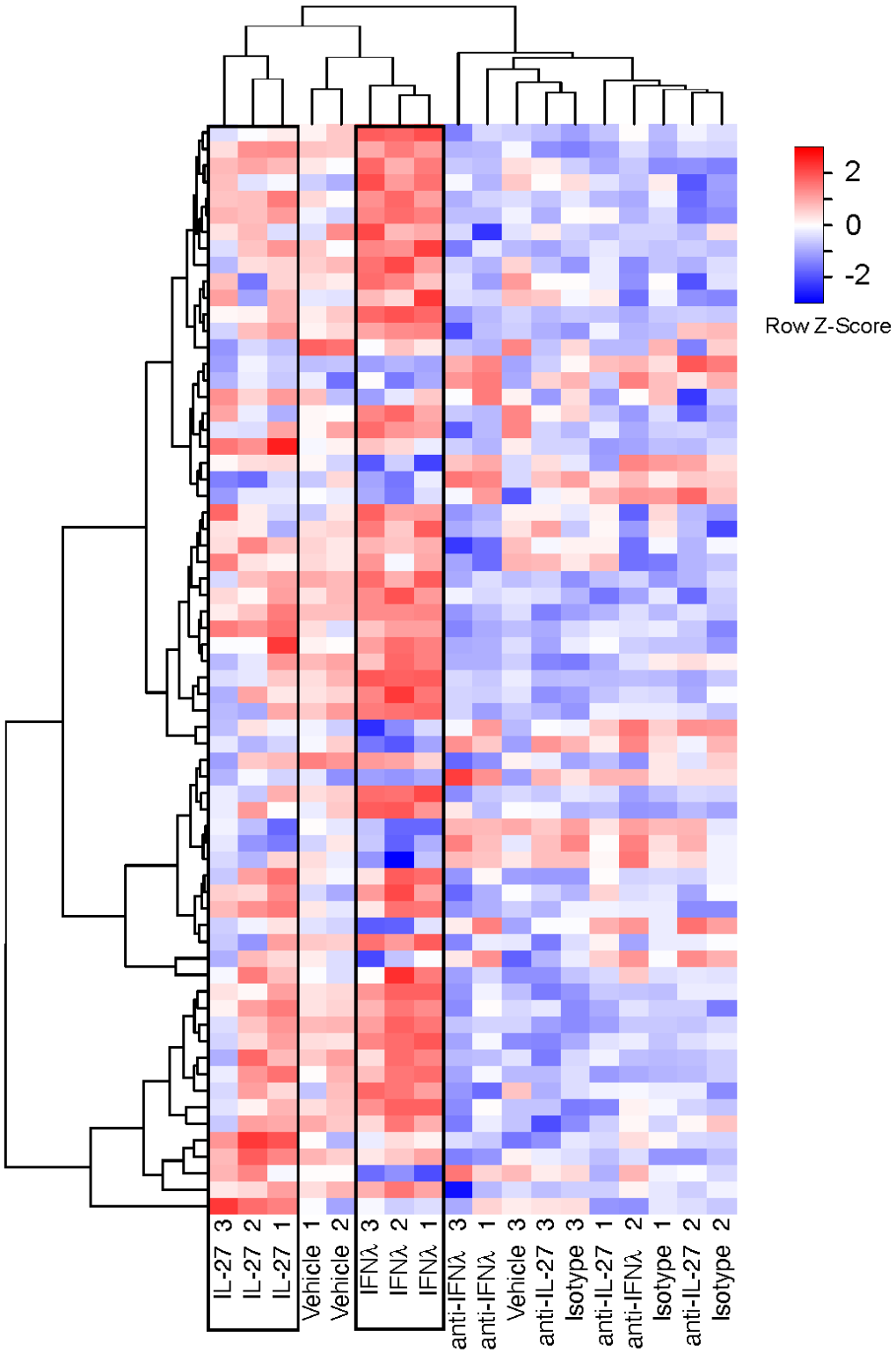

Supplemental Figure 3. Bulk RNA-sequencing of TOs

A. Heat map depicts gene expression data scaled by z-score for each row from bulk RNA sequencing of TOs. Columns represent samples clustered using Spearman correlation, and rows represent differentially expressed genes that were identified by comparing IL-27-stimulated to IL-27-neutralized TOs and IFNλ-stimulated to IFNλ-neutralized TOs, then clustered using Pearson correlation. 66 genes in the heatmap met cutoffs of p-value=0.05 and log fold-change=±0.5 and are listed in **Supplemental Table 2**. Data are representative of 3 independent samples per condition.

Supplemental Figure 4. p28 production within the murine labyrinth

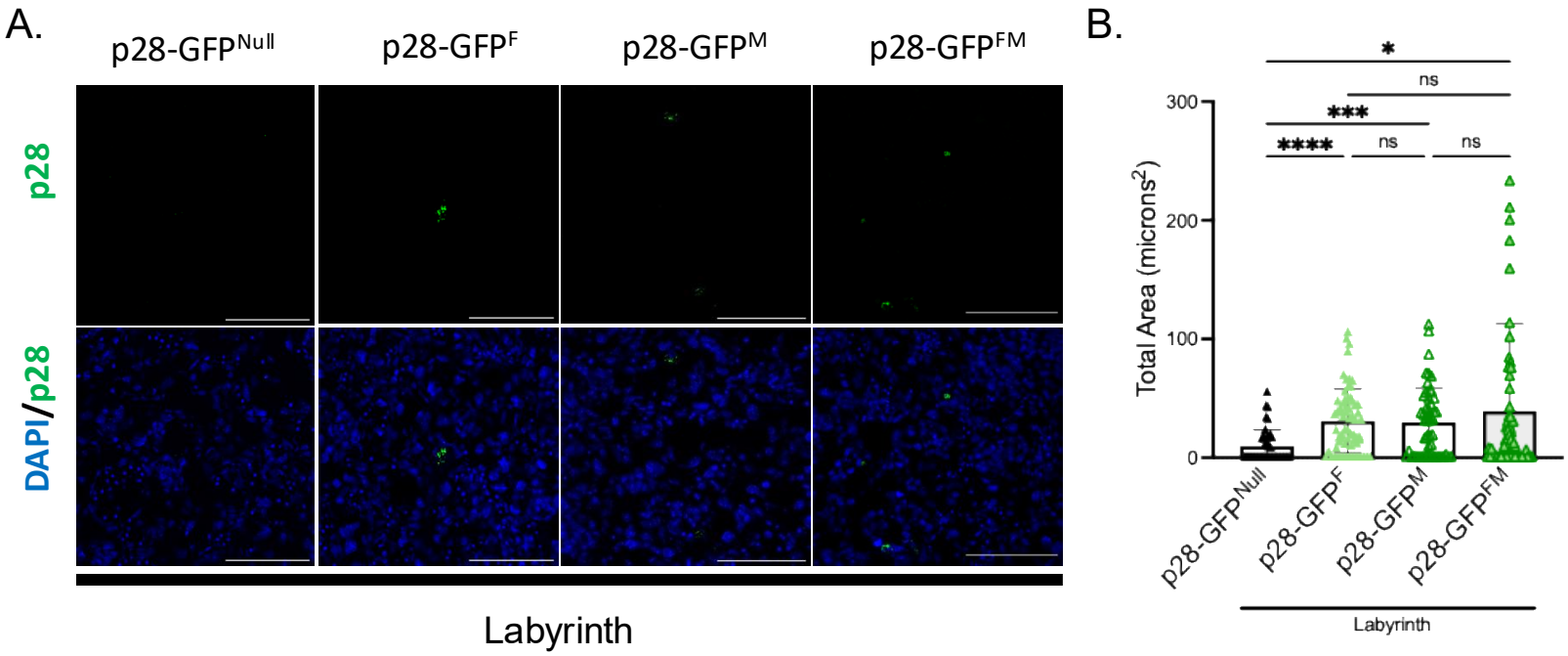

Supplemental Figure 4. p28 production within the murine labyrinth

A. p28-GFP localization within murine placental labyrinth at E13.5. 10µm placental cross-sections were stained with anti-GFP (green) and DAPI (blue) and imaged via microscopy. Representative images from 4 independent placentas. 20X magnification. Scale bar, 100µm.

B. Quantification of total labyrinth p28-GFP signal area (microns^2), as shown in **Figure 3E**, adjusted for scale. Graph represents measurements from 2-4 independent placentas per group, with 3-4 cross-sections obtained per placenta, and 4-8 images acquired per cross-section. Statistical analysis performed with Kruskal-Wallis ANOVA, *p<0.05, **p <0.001, ****p<0.0001.

Supplemental Figure 5. IL-27 signaling limits fetal pathology during murine congenital ZIKV infection

Supplemental Figure 5. IL-27 signaling limits fetal pathology during murine congenital ZIKV infection

A. Representative images of murine uterine horns isolated at E13.5 for tissue pathology and viral burden analyses. Black arrows highlight embryos exhibiting pathologic fetal outcomes.